River Flow 2010 - Dittrich, Koll, Aberle & Geisenhainer (eds) - © 2010 Bundesanstalt für Wasserbau ISBN 978-3-939230-00-7

3D near-bed flow field measurements at low sediment transport rates

M. Tregnaghi & S. Tait
School of Engineering, Design & Technology, University of Bradford, Chesham Building Richmond Road, BD7 1DP Bradford, UK

A. Bottacin-Busolin & A. Marion
Dept. of Hydraulic, Maritime, Environmental and Geotechnical Engineering, University of Padua, Via Loredan 20, I-35131 Padua, Italy

ABSTRACT: Experimental tests were carried out using a gravel bed in a tilting flume and a three camera 3D Particle Image Velocimetry (PIV) system. Sediment movement at variable transport rates was surveyed at the grain scale under uniform flow conditions. A natural river gravel with a well sorted sediment was used. This was subject to steady, uniform flows that generated a range of shear stresses that mobilized the sediment. 3D flow field measurements were made over a plane located few millimeters above the original sediment bed. Image processing and cross-correlation techniques were used to obtain high-resolution spatial and high-frequency temporal information of flow velocities. Sequences of images of the bed surface were taken simultaneously with the flow field measurements using an additional camera. An experimental approach is illustrated which links grain behavior with local velocity patterns. Such patterns of velocity can be either in terms of the three velocity components or in terms of the relevant time averaged Reynolds stresses. The potential is shown to develop statistically significant relationships which could describe the stochastic nature of sediment transport at different flow conditions.

Keywords: 3D PIV, Grain entrainment

1 INTRODUCTION

1.1 *Grain Motion and Sediment Transport*

The definition of a threshold for the initial motion of a grain has many consequences relevant to sediment transport. Following the early work of Shields (1936), the deterministic approach used to define conditions for the entrainment of sediments was widely accepted and used in common engineering applications. To date limited progress has been made to improve satisfactorily the physical understanding of the sediment transport close to threshold conditions. Many studies indicated discrepancies between thresholds estimated by Shields' criterion and observations. Two physical causes for such discrepancies have been suggested: the turbulent nature of the near-bed flow field and that the forces that resist motion are not a simple function of the submerged weight of grains. Field observations by Buffington et al. (1992) and Church et al. (1998) suggested that models that link entrainment simply to grain size may over predict sediment mobility because they ignore the contribution to bed stability caused by surface grain arrangements observed in water-worked deposits.

The state-of-the-art in sediment transport prediction consists of a wide range of equations, which all describe essentially the same phenomena. Although the underlying concepts used to develop these equations are different, the way in which these equations behave has certain common features (e.g. Gomez, 1991). Modelers still rely on empirically derived relationships, many of which were developed several decades ago to predict sediment entrainment and transport. Over the last ten years laboratory and field studies have started to provide some more detailed descriptions of water-worked deposits and the turbulent flows above them (Pilotti et al., 1997; Schuyler & Papanicolau, 2000; Munro et al. 2004). These observations have provided new insights into the physical processes that entrain grains in natural water. It is clear that fluvial sediment transport is caused by a complex interaction of many grain and fluid mechanic processes many of which are stochastic in nature and cannot therefore be adequately described by simple empirically calibrated deterministic equations. However, the modeling tech-

niques have not advanced by incorporating these new insights. Whilst there are empirical mixing layer models they suffer from the same drawbacks of the empirically calibrated bed-load transport rate formulae and cannot provide information on the time that particular sediments are retained within a deposit. Stochastic-based models, which rely on an understanding of the underlying particle mechanics within a water-worked sediment deposit have the potential to offer not only transport rate predictions but also this higher level information on the location and retention time of polluted sediment volumes.

Researchers are starting to move from empirically calibrated deterministic models where transported sediment is represented by average quantities to stochastic approaches to account for the random nature of the process. Modeling sediment dynamics at the grain scale is not only motivated by the need for addressing the uncertainties linked to classical sediment transport equations which represent natural stochastic processes in a spatial and temporal averaged manner but also to deal with new environmental needs. According to Grass (1970), the entrainment of sediments can be linked to the overlap of the probability distributions of the applied turbulent shear stress and the critical shear stresses to generate movement of particles. A number of recent studies have attempted to describe sediment entrainment by incorporating the probabilistic features of both the near bed turbulent flow and bed grain geometry (e.g. Papanicolau et al., 2001; Schmeeckle & Nelson, 2003). Wu & Chou (2003) and Wu & Yang (2004) described flow variability with probability distributions derived from literature and assumed the bed to be composed of randomly configured spheres. McEwan & Heald (2001) and Heald et al. (2004) used a discrete particle model and a normal distribution of the local flow field to predict the range of critical grain shear stresses. The main limitation of such approaches is that there is no data and few observations that link the entrainment of grains from water worked deposits with simultaneous measurements of the local flow velocities.

1.2 *Measurement Techniques*

Random variable analysis has been used, but a major limitation is the lack of appropriate data to test these models. Grain scale observation and multiple grain measurements have been achieved only recently as instrumental capabilities have improved. Increasing computational power has now created the potential to track and model each particle individually. However, this form of sediment modeling is now limited by the knowledge on the particle mechanics for natural grains rather than by computational limitations.

Some of the earliest experimental studies on the effect of turbulence on sediment entrainment were the laboratory studies of Grass, who showed that entrainment of fine grains could be linked with observed turbulent flow features. Drake et al. (1988) was one of the first studies to examine the motion of gravel particles entrained from a gravel river bed. They used high-speed motion picture to observe grain entrainments. Different grain behavior was noted for different size fractions, with smaller grains generally lifting from the bed and coarser particles rolling into motion. They also observed that the initiation of transport was characterized by short duration but localized periods of entrainment involving a number of grains. Although no measurements were made of the turbulent near-bed velocity field, this behavior was ascribed to ‘‘turbulent fluctuations’’ in the bed shear stress. Nelson et al. (1995) studied the interaction between turbulence events and bed load transport in the laboratory using LDA and a high-speed movie camera. By examining the statistics of the streamwise and vertical velocity fluctuations, u' and w', they concluded that ejections ($u' > 0$, $w' > 0$), which contribute negatively to the mean bed shear stress, moved sediment just as effectively as sweeps ($u' < 0$, $w' > 0$) which contribute positively to it. Other authors have stated that the pickup of sediments was found to be correlated to the instantaneous value of the streamwise velocity (Williams et al., 1989; Papanicolaou et al., 2001; Schmeeckle & Nelson, 2003). Schmeeckle et al. (2007) measured synchronously streamwise and vertical components of force on a near-bed spherical particle and the fluid velocity above or in front of it. They found that instantaneous drag force was not correlated with instantaneous Reynolds stress but strongly correlated with instantaneous streamwise velocity. Diplas et al. (2008) suggested that in addition to the magnitude of the instantaneous turbulent forces, the duration of these turbulent forces is also important.

The experiments described in the present paper were focused on the observations of the movement of single grains from deposits of natural gravel particles and the relevance of the local flow field. The experiments were therefore designed so that grain entrainments could be clearly identified and simultaneous measurements of the near-bed local flow field could be analyzed before any grain had been entrained. The aim is to provide the scientific community with a unique dataset in order to develop and validate techniques that can incorporate the stochastic entrainment of grains and reflect the erratic nature of grain motion once entrained.

2 THEORETICAL FRAMEWORK

2.1 *Experimental Approach To Grass' Theory*

According to Bottacin et al. (2008), Grass' joint probability approach has been reformulated to provide a framework which allow a direct experimental verification of the model. Findings reported above supports the assumption that the local near bed velocity u_f, rather than shear stress is the representative physical quantity affecting entrainment. This is a working assumption until complete analysis of the experimental data can clearly identify the physical mechanisms of entrainment and what variable probability distribution can be used to describe the mechanism. The velocity u_f is considered to be represented by a cumulative distribution F with probability density function f and the critical entrainment streamwise velocity u_g for individual grains to be represented by a distribution G with probability density function g (Figure 1). The probability of the critical entrainment velocity of a grain at an instant, u_g, lying within the interval δu centred at u is:

$$P\left(u-\frac{1}{2}\delta u \le u_g \le u+\frac{1}{2}\delta u\right)=g(u)\delta u \tag{1}$$

and the probability of u_f taking a value higher than u is given by:

$$P(u_f > u)=\int_u^{\infty} f(u)\,du = 1-F(u) \tag{2}$$

Assuming that u_g and u_f are statistically independent (Cooper & Tait, 2008), the joint probability of u_g lying within the range $u \pm \delta u/2$ and u_f taking a value higher than u gives the elemental risk of entrainment δR at an "instant" as:

$$\delta R(u) = g(u)\,\delta u\left[1-F(u)\right] \tag{3}$$

and therefore the risk density function is:

$$r=\frac{\delta R}{\delta u}=g\,(1-F) \tag{4}$$

The elemental risk $\delta R(u)$ represents the fraction of grains moved by a velocity lying in the range $u \pm \delta u/2$. However an entrainment "event" with a characteristic time scale t^* and a characteristic spatial scale l^* must be defined so that this can be scaled with the experimental observations of flow velocity and grain motion at entrainment. Evidence that particles move singly leads to identify the spatial scale with the grain size. The unit timescale must be associated with the flow features that entrain grains. Nino & Garcia (1996) suggested that the timescale covered by these features could be from 60÷80 time wall units (ν/u_*^2, where ν = kinematic viscosity and u_* = shear velocity) for small scale ejections to 1000÷1500 wall time units for the larger streamwise vortices. For flows over rough beds with u_* = 7÷8 cm/s, it follows ν/u_*^2 = $0.20\div0.15\cdot10^{-3}$ s. Experimental conditions presented in this study (see Table 1), which investigate bed load transport of coarse grains associated to large flow structures, suggest an "event" time scale of a few tenths of a second.

Assuming that the distributions g and F are stationary within a time interval Δt and that they apply uniformly over the observed bed surface, the probability density function of the critical streamwise velocity for the individual grains is given by:

$$g(u)=\frac{t^*}{\Delta t}\frac{r_e(u)}{1-F(u)} \tag{5}$$

where r_e = experimental risk density, which can be computed as:

$$r_e(u_i)=\frac{p_i}{\Delta u} \tag{6}$$

where p_i = fraction of superficial grains entrained given by:

$$p_i=\frac{N_{gi}}{N_{gs}} \tag{7}$$

Here N_{gi} = number of grains entrained by a velocity within the range $u_i \pm \delta u/2$ in the time interval Δt, and N_{gs} = number of grains on the bed surface exposed to the flow. This can be estimated as:

$$N_{gs}=\frac{A_{gs}}{\alpha\, l^{*2}} \tag{8}$$

where A_{gs} = total visible area of the observed superficial grains, l^* is equal to particle size, d, and α = shape factor, equal to 1 or $\pi/4$ depending on whether the area of a particle is approximated by a square or by a circle, respectively. Here A_{gs} = $(1-n)(L_x-2d)(L_y-2d)$, where n = bed porosity, and L_x and L_y = width of the area detected by the cam-

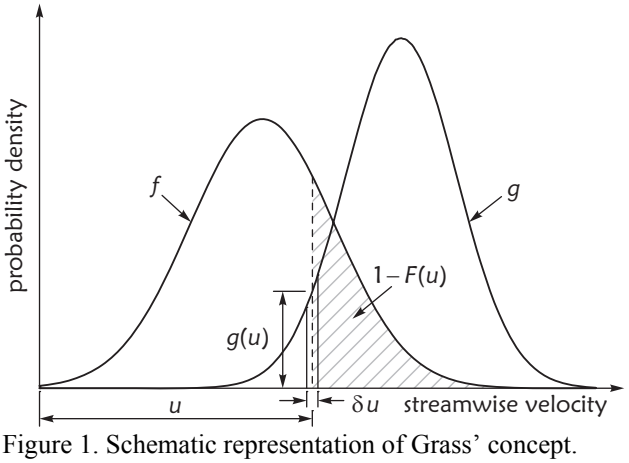

Figure 1. Schematic representation of Grass' concept.

eras in the x and y directions, respectively. This expression accounts for the fact that particles located at the edges of the area do not really contribute to the statistics.

The approach illustrated by Bottacin et al. (2008) shows how to derive the experimental probability distributions of the critical velocities required to entrain grains. Using the measured distributions of streamwise velocity $f(u)$ and the flow velocities at entrainment $r_e(u)$ it is possible to estimate a section of the probability density function of the critical streamwise velocities for the sediment bed. However, the extent of the curve section is strongly dependent on the degree of overlapping between the *pdf* of the local and critical velocities, respectively. This can be only a small part of the total distribution if flow conditions are just above the critical threshold for sediment motion. In order to obtain a full description of such curves based on the revised Grass approach, data analysis must be performed considering steady-state flows characterized by increasing values of the average bed shear stress.

2.2 *2D Flow-Field Measurements*

Bottacin et al. (2008) carried out experiments using a mobile gravel bed placed in a tilting flume with a modified 2D particle image velocimetry (PIV) system. The analysis of the collected images identified a number of near-bed velocity ‘‘signatures’’ linked to grain movement. Changes of the time averaged local velocities were observed when sediments were entrained or deposited by the flow. Results showed that about 60% of the identified grain displacements were associated to one or more patterns of the near-bed velocity data. Among this subset, most of cases revealed correlations with the time-averaged streamwise and lateral velocities $\overline{u}$ and $\overline{v}$ (55% and 39%, respectively). Only a relatively small number of the cases were associated to changes of the streamwise and transverse fluctuations $u'u'$ and $v'v'$ (27% and 22%, respectively) and to changes of the cross product $u'v'$ (12%), which is related to the Reynolds stress.

It was then argued that grain-scale changes of the bed surface affect more significantly the local velocity than the other flow quantities, while grain movements are much more poorly correlated to Reynolds stress. The reported analysis was limited to velocity data in the 2D plane, and did not identify correlations between instantaneous velocities and grain motion, possibly due to the low sampling frequency (9Hz). Further analysis is therefore needed to examine the flow statistics and correlations of the streamwise and vertical near-bed velocities associated to grain movement.

3 EXPERIMENTAL DESIGN

The experiments were conducted in the Hydraulics Laboratory at the University of Bradford. A 12m long, 0.5m wide tilting flume was equipped with state-of-the-art monitoring system that enabled high resolution velocity measurement of free surface flows over rough boundaries and sediment fluxes at high spatial resolutions. A fixed bed made of gravel glued on a plastic surface covered the upstream end of the flume for a distance of 1.50 m. This ensured the uniform development of a stable upstream boundary layer for all experiments. The remaining part of the flume was filled with loose natural river gravel ranging from 1 to 10 mm, with average diameter d_{50} = 5.5 mm, standard deviation σ_g = 1.3, and density ρ_s = 2650 kg/m^3 (see Figure 2). This sediment was well mixed, placed in the flume and scrapped flat using a mechanically scrapper. This produced a well mixed flat sediment deposit of a uniform thickness and no bed forms. Afterwards, the flume was tilted reaching the desired slope and a constant water discharge was imposed. Hydraulic conditions were above the threshold of grain motion. A uniform flow condition was obtained by adjusting a weir placed at the downstream end of the flume. Hydraulic conditions were selected so that individual grain entrainments and depositions could be clearly identified and measured velocity perturbations could be unambiguously linked to individual grain events.

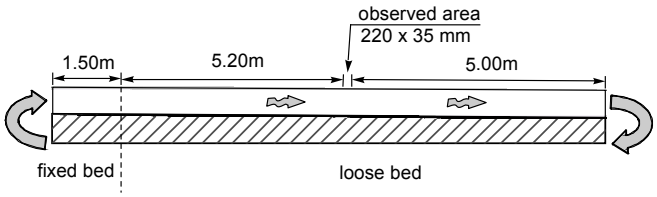

Figure 2. Longitudinal section of the flume.

The 3D Particle Image Velocimetry System (PIV) was designed to measure 3D flow velocities in a single plane. The laser illumination, timings for the two cameras and the data acquisition were all controlled by a single PC. Images were acquired direct to a RAID array of hard drives so that the system was capable of measuring flow velocities at a frequency of up to 45Hz for several minutes. The PC controlling the PIV system was linked to another PC that drove a fast video camera. The fast video camera could acquire bed images at rates up to 200Hz, and operate for several minutes at the highest sampling rates. The bed was illuminated by a high-speed strobe light, so that by use of a careful selection of camera, laser and strobe timings it was possible to eliminate cross-talk between the bed and the PIV cameras.

By combining this system with the PIV system, measurements on grain movements were obtained that could be linked with 3D flow velocity measurements. The observed area and the sides of the flume adjacent to the measurement area were obscured to reduce the ingress of any external light so as to improve the consistency of the quality of the images and for safety reasons. A platform was build next to the tilting flume so that the pulsed laser position could be adjusted and a pulsed light sheet could be generated and located a few millimetres above the gravel bed surface. Two pulsed lasers generated a high-intensity green light beam. Beam-expanding optics placed at the side of the flume produced a green light sheet of approximately uniform intensity which was located parallel and approximately 10 mm above and parallel to the original sediment bed.

An area of 220 mm by 40 mm located on the centreline of the flume was selected for measurement. This area was viewed by the three cameras placed vertically above the water surface (see Figure 3). A floating glass sheet was placed at the same level as the design water depth to avoid water surface oscillations interfering with the focus of the cameras on the investigation area. The area size was selected to provide velocity data at a suitable spatial scale (one interrogation area to correspond to approximately one grain), and the area was large enough so that enough grain motions could be observed in an experiment so that statistically significant data on grain entrainment could be obtained. Two cameras had a green filter and the other operated under white light conditions. The cameras with the green filter were used to obtain flow field information whilst the other camera was used to gather data on grain entrainment, depositions and movements. They collected pairs of images with the time step between the images Δt_p = 1 ms and the frequency of the collection of image pairs f_r = 45 Hz.

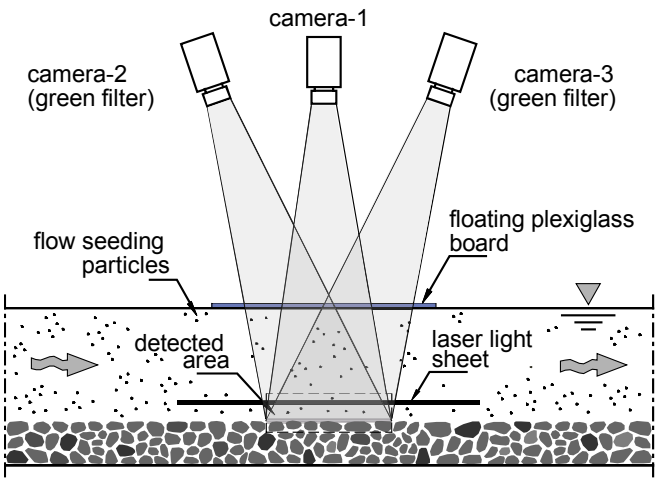

Figure 3. Modified PIV measurement system.

The images recorded the "instantaneous" positions of the flow tracing particles. In order to measure the spatial flow velocity pattern, seeding particles were fed into the flow. These particles were polystyrene spheres with an average size of d_p = 200 μm and density ρ_p = 995 kg/m^3. Their low submerged density and inertia meant that they closely followed the flow. Camera-1 was focused on the sediment bed surface, it was illuminated by a white strobe light and captured an image of the bed at the starting time of the second pair images recorded by cameras-2 and -3. Bed images were also collected at a 45 Hz frequency (Figure 4). This set-up provided velocity data sets with a spatial resolution that was comparable to the grain scale. This was done so that velocities at particular locations could be associated with the movement of individual grains. Flow velocity and grain motion measurements were taken simultaneously for periods of approximately 10 minutes of duration during each test. Each recording section acquired nearly 27,000 x 5 images, which were temporarily stored into the acquisition buffer and then transferred into the stored database.

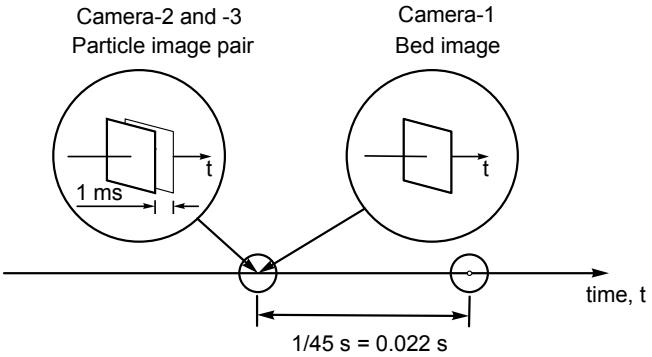

Figure 4. Timing of the image acquisition system.

Data from 12 tests carried out at different slopes but with similar water depths, h = 10 cm, are reported. Table 1 shows the main hydraulic parameters of the experimental tests: S = slope of the flume, approximately equal to the bed slope during the recording session; Q = water discharge; U = flow velocity averaged over the flow cross sectional area; $R_e = 4R_HU/\nu$ = flow Reynolds number, where R_H = hydraulic radius; $u_* = (gR_HS)^{0.5}$ = average bed shear velocity, where g = acceleration due to gravity; and $\tau_* = \tau_0/g(\rho_s-\rho)d_{50}$ = Shields' parameter, where τ_0 = mean bed shear stress and ρ_s and ρ = density of sediment and water respectively. The experiments were run with increasing levels of boundary shear stress, so that the distribution of velocities and linked grain motions can be determined as the system moves away from the threshold of motion (τ_* = 0.057) to conditions of well developed bed-load transport (τ_* = 0.090).

Table 1. Hydraulic parameters for experimental tests

Test	S(%)	Q(l/s)	U(m/s)	$R_e(\cdot 10^5)$	u_*(m/s)	τ_*(-)
01	0.55	40.5	0.88	2.81	0.067	0.057
02	0.57	42.6	0.93	2.93	0.069	0.059
03	0.59	43.3	0.94	2.98	0.070	0.061
04	0.62	43.8	0.95	3.02	0.071	0.064
05	0.65	44.8	0.97	3.10	0.074	0.068
06	0.69	45.6	0.99	3.16	0.076	0.072
07	0.72	46.4	1.01	3.22	0.077	0.074
08	0.75	47.2	1.03	3.28	0.079	0.077
09	0.77	48.1	1.05	3.34	0.080	0.080
10	0.80	49.0	1.07	3.40	0.081	0.083
11	0.83	49.8	1.08	3.45	0.083	0.086
12	0.86	50.9	1.11	3.53	0.085	0.090

4 FLOW FIELD AND GRAIN MOTION

4.1 *3D Near-Bed Velocity*

Flow-field images were used to obtain the three velocity components, u, v and w, and the relevant cross-products $u'v'$ and $u'w'$. The observed area was split into many 4.30 mm × 4.30 mm "interrogation areas" with an overlap of 75% of these areas both in streamwise and lateral directions. Cross-correlation of each interrogation area between paired images allowed the local fluid displacement to be estimated. This combined with information on the time interval between the paired images allowed spatial velocity fields to be obtained. The velocities of the fluid were therefore known on a 1.15 mm square mesh grid, with N = 35×185 = 6475 nodes. This set-up provided velocity data sets with a spatial resolution that was comparable to the grain scale.

The temporal trend of the flow field velocities in the proximity of the moved grains were collated from the flow field data and used by linking the locations of grain motion with the local velocity patterns, e.g. streamwise velocity (Figure 5a). Data analysis focused on time periods > 10s (about 900 data points) before grains were entrained. The *pdf* of such velocity samples were investigated and a "match" with an entrainment event was assumed to occur if the flow velocity fell above the 85th percentile of the relevant *cdf* (Figures 5b and c). A bounding box was created around the boundary of the grains under investigation to approximate their spatial extent (Figure 6). The velocity measurements at points within and immediately adjacent to the bounding box were found to have similar values, indicating spatial flow structures comparable to or larger than grain size. Preliminary results from three experiments on few hundred grains indicated that about 70% of entrainment events were associated to peak values of the streamwise velocity u, For 20% of cases the streamwise velocity was found around average or below, but they were associated to high fluctuations of lateral or vertical components, v and w. This evidence suggests a strong link between grain motion and local drag with some combination of lift or lateral destabilizing forces, as supported by direct observations of bed images during the first instants of the movement. Reynolds stresses were found to have weak correlations with grain entrainment. The remaining part of the sample was not found to be significantly associated to any flow signature. However, in some cases closer inspection of data suggests that these grains were possibly put in motion by other particles passing through their neighbourhood, or leaving their position few diameters upstream thus reducing the sheltering effect.

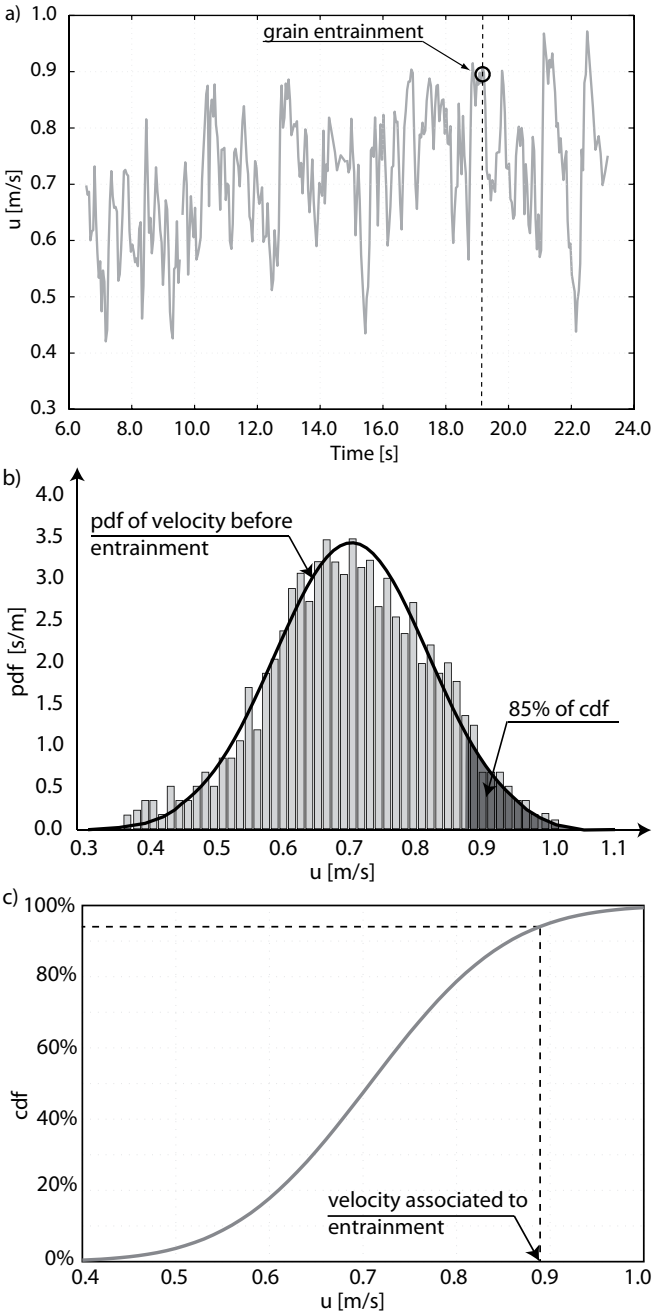

Figure 5. Near-bed flow field and grain motion: a) velocity time-series before grain entrainment; b) velocity pdf and 85th percentile of cdf; c) velocity at entrainment.

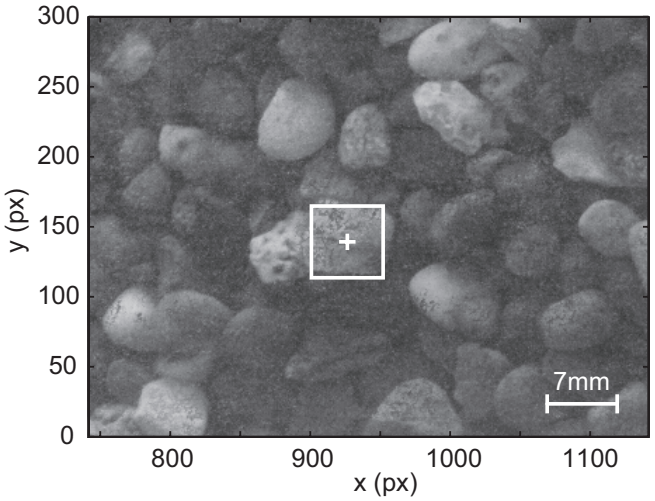

Figure 6. Image of the bed surface. Identification of moving grains (bounding box).

4.2 *Potential for Analysis*

The experiments were designed moving from threshold conditions for grain entrainment to developed transport conditions. This was done as the measure of the probability density function of the critical streamwise velocities for the sediment deposit is strongly dependent on the degree of overlapping between the *pdf* of the local and critical velocities, respectively (see Figure 1). The analysis of the new dataset, based on the revised Grass approach, can lead to a full description of such curves. The main limitation of the method is that the higher the transport rate the more difficult is the identification of individual entrainment events through visual image techniques. Hydraulic conditions were selected so that grain movements could be clearly identified and linked to local near-bed velocities. On the other hand, the imposed shear stresses induced levels of sediment transport which in principle guarantee the measurement of a significant segment of the critical velocity *pdf* for the sediment deposit. Further, for low-rate sediment transport the effects of turbulent fluctuations are more significant than those associated to temporal average values.

The method illustrated in Section 2.1 is currently being applied to the experimental data, by combining the velocity and grain entrainment measures described in this paper. The purpose is to verify the theoretical approach by Grass and validate the experimental method itself. If the sections of the probability density function $g(u)$ obtained at different transport rates will overlap (see Figure 7), then the approach will be validated. This means that a unique description of the resistance of grains to flow action exists, which depends on grain characteristics and local bed texture. Armoring and selective sediment transport occurs for natural sediment beds (e.g. Marion et al., 2003), this may affect the bed characteristics during time. However, the limited time of the recording session and the use of well sorted sediment should guarantee similar sediment bed composition and arrangement in all the experiments. This is also supported by findings of Cooper & Tait (2008) who found that the spatial pattern of near-bed velocities did not have a strong correlation with bed topography at the grain-scale.

To apply Eq. (5) to the experimental data it is also necessary to estimate a suitable time scale t^*. In the experiments carried out by Bottacin et al. (2008) the frequency of the PIV images was not sufficient to identify unambiguously the duration of the flow feature that entrained grains. Given that entrainment of bed load that was investigated, time scale of the order of a few tenths of a second was considered reasonable (e.g. Nino & Garcia, 1996). However, some uncertainties still remain about the choice of such temporal parameter, which can sensibly affect the final estimate.

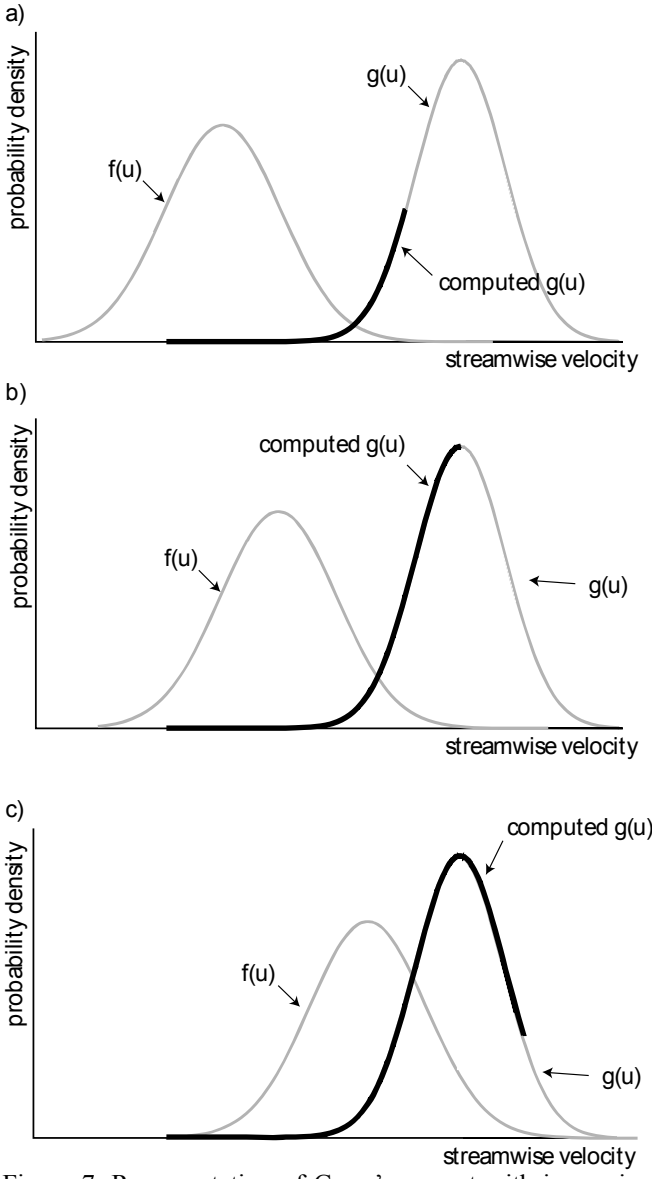

Figure 7. Representation of Grass' concept with increasing level of transport: a) threshold conditions; b) low sediment transport rate; c) developed sediment transport.

5 CONCLUSIONS

A new experimental design has been described that allows to collect high spatial and temporal resolution images of mobile beds that can be linked with 3D near-bed flow velocity fields. The collected data will be used to obtain an experimental measure of the probability density function (*pdf*) of the boundary shear stress at threshold conditions. Grass' joint probability approach is proposed to gain insight into the physical nature of entrainment and transport processes. Using the measured distributions of streamwise velocity $f(u)$ and the flow velocities at entrainment it is possible to estimate a section of the probability density function $g(u)$ of the critical streamwise velocities for the sediment deposit. This is a statistical measure of the "strength" of a bed. Determining such distributions in other ways is not possible. The purpose is demonstrating that if information is available then grain entrainment rates can be predicted stochastically. Inferring the probability density of the boundary flow velocity needed to dislodge the sediments based on a distribution of grain exposures and fluid velocities would be an important advance in understanding grain entrainment processes, which is the basic process relevant to all sediment transport predictions. This can be accomplished by comparing the *pdf* of the measured near-bed flow velocity fields with the *pdf* of the flow velocity characteristic that is linked with a grain entrainment.

REFERENCES

Bottacin-Busolin, A., Tait S.J., Marion A., Chegini A., Tregnaghi M. 2008. Probabilistic description of grain resistance from simultaneous flow field and grain motion measurements. Water Resour. Res., 44, W09419, DOI: 10.1029/2007WR006224.

Buffington, J.M., Dietrich W.E., Kirchner J.W. 1992. Friction angle measurements on a naturally formed gravel streambed: Implications for critical boundary shear stress. Water Resour. Res., 28(2), 411–425, DOI: 10.1029/91WR02529.

Cooper, J.R., Tait S.J. 2008. The spatial organization of time-averaged streamwise velocity and its correlation with the surface topography of water-worked gravel beds. Acta Geophysica 56(3), 614-641, DOI: 10.2478/s11600-008-0019-9.

Church, M., Hassan M., Wolcott J.F. 1998. Stabilizing self organized structures in gravel-bed stream channels: Field observations and experimental observations. Water Resour. Res., 34(11), 3169–3179, DOI: 10.1029/98WR00484.

Diplas, P., Dancey C.L., Celik A.O, Valyrakis M., Greer K. and Akar T. 2008. The role of impulse on initiation of particle movement under turbulent flow conditions, Science, 322, 717-720, DOI: 10.1126/science.1158954.

Drake, T.G., Shreve R.L., Dietrich W.E., Whiting P.J., Leopold L. 1988. Bedload transport of fine gravel observed by motion picture. J. Fluid Mech., 192, 2193–2217, DOI: 10.1017/S0022112088001831.

Grass, A.J. 1970. Initial instability of fine sand. J. Hydraul. Div., 96(3), 619–632.

Gomez, B. 1991. Bedload Transport. Earth Science Reviews, 31, 89-132.

Heald, J., McEwan I., Tait S.J. 2004. Sediment transport over a flat bed in a unidirectional flow: Simulations and validation. Philos. Trans. R. Soc., 362, 1973–1986.

Marion, A., Tait S.J., McEwan I K. 2003. The analysis of small-scale gravel bed topography during armouring. Water Resour. Res., 39(12), 1334, DOI:10.1029/2003WR002367.

McEwan I., Heald, J. 2001. Discrete particle modeling of entrainment from flat uniformly sized sediment beds. J. Hydraul. Eng., 127 7), 588-597.

Munro, R.J., Dalziel S.B., and Jehan H. 2004. A pattern matching technique for measuring sediment displacement levels. Exp. Fluids, 37(3), 399–408, DOI: 10.1007/S00348-004-0829-8.

Nelson, J. M., Shreve R.L., McLean S.R., Drake T.G. 1995. Role of near bed turbulence structure in bed load transport and bed mechanics, Water Resour. Res., 31(8), 2071–2086.

Nino, Y., Garcia M. H. 1996. Experiments on particle turbulence interactions in the near wall regions of an open channel flow: Implications for sediment transport. J. Fluid Mech., 326, 285–319, DOI: 10.1017/S0022112096008324.

Papanicolaou, A., Diplas P., Dancey C., Balakrishnan M. 2001. Surface roughness effects in near-bed turbulence: Implications to sediment transport. J. Eng. Mech., 127(3), 211–218.

Pilotti, M., Menduni G., Castelli E. 1997. Monitoring the inception of sediment transport by image processing techniques. Exp. Fluids, 23(3), 202–208, DOI:10.1007/s003480050103.

Schuyler, A., Papanicolau A. 2000. Image analysis technique to track the evolution of sediment clusters. J. Exp. Tech., 24(5), 31–36.

Schmeeckle, M.W., Nelson J.M. 2003. Direct numerical simulations of bed load transport using a local, dynamic boundary condition. Sedimentology, 50(2), 279–301, DOI: 10.1046/j.1365-3091.2003.00555.x.

Schmeeckle, M.W., Nelson J.M., Shreve R.L. 2007. Forces on stationary particles in near-bed turbulent flows. Water Resour. Res., 112, F02003, DOI: 10.1029/2006JF000536.

Williams, J.J., Thorne P.D., Heathershaw A.D. 1989. Measurements in the benthic boundary layer over a gravel bed. Sedimentology, 36(6), 959–971, DOI: 10.1111/j.1365-3091.1989.tb01533.x.

Wu, F.C., Chou Y.J. 2003. Rolling and lifting probabilities for sediment entrainment. J. Hydraul. Eng., 129(2), 110–119.

Wu, F.C., Yang K.H. 2004. Entrainment probabilities of mixed size sediment incorporating near bed coherent flow structures. J. Hydraul. Eng., 130(12), 1187–1197.